The Journal of Chemical Physics

RESEARCH ARTICLE | DECEMBER 11 2024

CO adsorption on CeO_2(111): A CCSD(T) benchmark study using an embedded-cluster model

Juana Vázquez Quesada ; Sarah Bernart ; Felix Studt ; Yuemin Wang ; Karin Fink

J. Chem. Phys. 161, 224707 (2024)
https://doi.org/10.1063/5.0231189

The Journal of Chemical Physics ARTICLE pubs.aip.org/aip/jcp

CO adsorption on CeO_2(111): A CCSD(T) benchmark study using an embedded-cluster model

Cite as: J. Chem. Phys. 161, 224707 (2024); doi: 10.1063/5.0231189
Submitted: 29 July 2024 • Accepted: 1 November 2024 •
Published Online: 11 December 2024

Juana Vázquez Quesada,[1,a] Sarah Bernart,[2] Felix Studt,[2] Yuemin Wang,[3] and Karin Fink[1]

AFFILIATIONS

[1] Institut für Nanotechnologie, Karlsruher Institut für Technologie (KIT), Kaiserstraße 12, 76131 Karlsruhe, Germany
[2] Institut für Katalyseforschung und Technologie, Karlsruhe Institut für Technologie (KIT), Kaiserstraße 12, 76131 Karlsruhe, Germany
[3] Institut für Funktionelle Grenzflächen, Karlsruher Institut für Technologie (KIT), Kaiserstraße 12, 76131 Karlsruhe, Germany

[a] **Author to whom correspondence should be addressed:** juana.quesada@kit.edu

ABSTRACT

A benchmark model that combines an embedded-cluster approach for ionic surfaces with wavefunction-based methods to predict the vibrational frequencies of molecules adsorbed on surfaces is presented. As a representative case, the adsorption of CO on the lowest index non-polar and most stable facet of CeO_2, that is, (111) was studied. The CO harmonic vibrational frequencies were not scaled semiempirically but explicitly corrected for anharmonic effects, which amount to about 25 cm^{-1} with all tested methods. The second-order Møller–Plesset perturbation method (MP2) tends to underestimate the CO harmonic frequency by about 40–45 cm^{-1} in comparison with the results obtained with the coupled-cluster singles and doubles with perturbational treatment of triple excitation method [CCSD(T)] and independently from the basis set used. The best estimate for the CO vibrational frequency (low-coverage case) differs by 12 cm^{-1} with the experimental value obtained by infrared reflexion absorption spectroscopy of 1 monolayer CO adsorbed on the oxidized CeO_2(111) surface. In addition, a conservative estimate of the adsorption energy of about −0.22 ± −0.07 eV obtained at the CCSD(T) level confirms the physisorption character of the adsorption of CO on the CeO_2(111) surface.

I. INTRODUCTION

For a molecule adsorbed on a crystal surface (low-coverage case), periodic calculations require a large supercell that minimizes the interactions between the adsorbate and its periodic pattern, which renders computations extremely demanding especially when using hybrid functionals. An alternative strategy to locally study thermodynamic or kinetic processes in periodic systems is to consider a part of a limited size, the so-called quantum-mechanical (QM) cluster, where the phenomenon under study takes place. Finite clusters allow studying isolated defects and adsorbates with a lower computational cost and simultaneously enable the use of systematically converging and accurate post-Hartree–Fock methods establishing the path toward predictions with a level of accuracy closer to that achieved for molecules in gas phase. Nevertheless, the main disadvantage of this approach is that it is a finite truncated model in which long- and medium-range interactions between the cluster and its surroundings are neglected. A way, however, of solving the aforementioned limitation is the use of embedding schemes, which represent the periodic system in a certain manner.

During the past few decades, different embedding models have been developed when working with periodic systems (bulk and surfaces) and when studying the adsorption of molecules in different facets of ordered crystals (see, for example, Ref. 1). The fragment of interest, the QM cluster, is treated for correlation effects while being embedded, either in a system defined employing plane wave-based periodic Density Functional (DF)[2–4] or Hartree–Fock (HF)[5,6] theory, or in a system described by periodic wavefunction based

HF.[7–10] The so-called *Watson sphere*[11] was the origin of a different family of embedding schemes used for ionic systems (e.g., some oxides) in which the environment effects in the QM cluster are shaped by creating a series of point charges (PCs). The difference between the various PC-designs is based on how the charges are distributed around the QM cluster, how they are truncated in a finite set, and which charge values are chosen. On that account, various techniques and models have been proposed in order to achieve rapid and correct convergence to the Madelung potential (see, for example, Refs. 12–14). These latter issues have often been addressed by including additional charges such as originally proposed by Evjen[15] as well as by Piela *et al.*[16,17] In all cases, the periodic system is divided into a local region (QM cluster), which is treated with a quantum chemical method—usually a post-Hartree–Fock method—and the surroundings of the crystal, described by an electrostatic potential consisting of a grid of point charges. In addition, a boundary region can be created to isolate the charge field from the QM cluster to avoid overpolarization of the cluster or charge transfer to the point charge field.[18,19] In this boundary region, the positive point charges are replaced by pseudopotentials [effective core potentials (ECPs)], which generally simulate, to a certain extent, the exchange repulsion effect and compensate for polarization. Resuming the use of this electrostatic embedding model, recent studies have determined, for example, the adsorption energies of small molecules on the rutile TiO_2(110) (H_2O, NH_3, CH_4, CH_3OH, and CO_2)[20] and MgO(001) (CO)[21] surfaces and investigated oxygen vacancies in metal oxides.[22,23] Among these recent developments, the periodic electrostatic embedding cluster model (PEECM)[24] is meant to be used in an automated manner.[25,26]

In conjunction with these general schemes, computational challenges arise when dealing with rare earth oxides, which are becoming increasingly important in catalysis and technological development.[27–29] Among them, cerium dioxide (CeO_2, ceria) represents perhaps the most significant example.[30,31] The importance of ceria in catalysis is due to its capacity to store oxygen, i.e., its ability to serve as a support or catalyst for redox cycles in different reaction stages. The investigation of reaction mechanisms that take place on ceria surfaces or on those where ceria acts as a support requires the use of experimental techniques that provide sufficient sensitivity to distinguish diverse surface orientations and eventually the presence or absence of vacancies and dopants.[32,33] The surface-ligand infrared (IR) vibrational spectroscopy (SLIR)[34] in conjunction with carbon monoxide (CO) as a probe molecule has proved to be very sensitive to the structure of oxide surfaces.[35–39] However, the assignment of the bands in the range between 2150 and 2180 cm^{-1} has been a topic of discussion for years, being identified with the stretching vibration of CO bound to a hydroxyl group or adsorbed on Ce^{4+} with more or less close oxygen vacancies.[40–42] To that matter, theoretical studies that try to explain and confirm the experimental evidence face a case of physisorption, i.e., a weakly bound molecule,[43] where the prediction of the binding energy as well as the vibrational frequency of CO with a particular degree of accuracy represents a great endeavor, maybe even more acute than in other systems with other interaction types linking the molecule more strongly to the surface. All the latter and its ease enabling the creation and stabilization of oxygen vacancies[44] has motivated multiple studies using periodic density functional theory (DFT), many of them carried out by Ganduglia-Pirovano *et al.* (see Refs. 45 and 46 and references therein) with recent contributions providing the most exhaustive studies.[47–49]

Electrostatic embedding models have also been applied in few occasions to CeO_2 bulk[24,50] as well as the (111)[14,24,51] and (110)[52–56] low-index surfaces, which sometimes included the estimate of the CO binding energy on the (110)[52,54–56] and (111)[14,51] surfaces. For this latter purpose and in the case of CO@CeO_2(111),[51] an embedded $Ce_{13}O_{26}$ (111) cluster was used in which all six coordinates of the CO molecule were optimized employing the B3LYP functional and subsequent second-order Møller–Plesset perturbation theory (MP2) and coupled-cluster singles and doubles with perturbational treatment of triple excitation method [CCSD(T)] single-point calculations were accomplished in order to apply the method of increments.[57–59]

To the best of our knowledge, post-Hartree–Fock methods such as MP2 and CCSD(T) have never been applied for the prediction of the vibrational frequency of CO molecule, adsorbed on CeO_2 surfaces. Although the idea of applying methods such as CCSD and CCSD(T) to materials by imposing periodic boundary conditions has been promoted over the past decade (see Refs. 60–62 and references therein), the high computational cost has limited their routine use. Therefore, different reduced-scaling techniques—for example, the local natural orbital (LNO) coupled-cluster (CC) method (LNO-CC)—has been developed and applied intensively; see Ref. 10 for a compact summary.

Thus, this work benchmarks, for the first time, the stretching frequency of CO adsorbed on the (111) facet of CeO_2, as well as its binding energy by means of the embedding cluster model PEECM in conjunction with correlated methods such as MP2 and canonical CCSD(T). In addition, unlike common practice in theoretical catalysis,[47] the CO harmonic vibrational frequencies were not scaled semiempirically but explicitly corrected for anharmonic effects utilizing a one-dimensional representation of the anharmonic potential along the CO vibrational normal coordinate.

The rest of this paper is organized as follows: Sec. II describes the details of the methodology applied in this work. The presentation and discussion of the results are elaborated in Sec. III. The influence of the size and shape of the clusters used in the embedding model when predicting the frequency of the CO is analyzed in Sec. III A. Section III B focuses on the analysis of the computed CO stretching frequency and on the assessment of the origin and magnitude of the uncertainties of the predicted values. In addition, in this section and in the aftermath of including anharmonic corrections, the final results are compared with the experimental evidence. Next, the CO binding energy is evaluated and compared to the previous literature (Sec. III C). Finally, Sec. IV summarizes the present work indicating the possibility of applying the methodology reported here to other cases where other CeO_2 facets are studied—including the presence of oxygen vacancies—as well as other adsorbates and catalytic processes for which an accurate theoretical prediction can play an important role.

II. METHOD

A. Surface structural optimization by periodic DFT

Five different computed CeO_2(111) surfaces taken from the literature or optimized in this work were investigated. In all cases, the slab layer model and the supercell approach,[63] in conjunction

with the Vienna *Ab initio* Simulation Package (VASP),[64,65] were employed. These surfaces were obtained using three different functionals, i.e., the van der Waals functional BEEF-vdW,[66] the PBE[67] functional, within the generalized gradient approximation (GGA), in conjunction with a Hubbard U-like term[68] (U = 4.5 eV for the 4f states of Ce), and the HSE06 hybrid functional.[69–74] Bulk ceria has a structure belonging to the Fm3m space group with calculated lattice constants of 5.499 Å (BEEF-vdW), 5.485 Å (PBE + U),[48] and 5.398 Å (HSE06).[48] The CeO_2(111) structure obtained with the BEEF-vdW functional with a slab model consisting of (2 × 2) layers was directly computed in this work, while the data regarding the PBE-U and HSE06 functionals and employing the cell sizes of (1 × 1) and (2 × 2) were taken from the literature.[48] In all cases, the Monkhorst–Pack[75] method was used to explore the Brillouin zones. All supercells were defined with a vacuum space of at least 15 Å. The valence electrons [Ce(4f, 5s, 5p, 5d, 6s) and O(2s, 2p)] were treated with the projector augmented wave (PAW) method with a wave cutoff energy of 500 eV (415 eV for the BEEF-vdW calculations). The remaining electrons were treated as part of the atomic cores.

B. Embedded cluster model and post-Hartree–Fock methods

All embedded computations were performed using the TURBOMOLE program package.[76] Second-order Møller–Plesset perturbation theory (MP2)[77] as well as the coupled-cluster singles and doubles with perturbational treatment of triple excitation [CCSD(T)][78] methods were considered in this research, employing the Karlsruhe def2-SVP, def2-TZVPP, and def2-QZVPP basis sets,[79,80] as well as the aforementioned basis sets with the inclusion of a small number of moderately diffuse basis functions, i.e., def2-SVPD, def2-TZVPPD, and def2-QZVPPD.[81,82] The resolution-of-the-identity approximation (also called density fitting) was applied in all post-Hartree–Fock methods using optimized auxiliary basis sets.[81,83–85] In the case of cerium and the D basis sets, the auxiliary basis sets were constructed applying the procedure described in Ref. 86. All "def2" basis sets for cerium contain a scalar-relativistic effective small core potential (ECP) of the Wood–Boring (WB) type covering the inner 28 electrons.[87] Convergence thresholds of $10^{-10}E_h$ and $10^{-10}E_h/a_0$ were specified for the self-consistent field energies and Cartesian gradients, respectively.

For the iterative solution of the coupled-cluster equations, both the change in the energy with respect to the previous iteration and the Euclidean norm of the residual were chosen to be smaller than 10^{-10}. These tight settings had significant repercussions on the number of iterations for the solution of the coupled-cluster equations and on the cost for individual iterations, although they were absolutely necessary to guarantee an accuracy better than 0.5–0.1 cm^{-1} for the vibrational frequencies computed from numerical first and/or second derivatives of the potential energy. For most of the post-HF methods, the core electrons were not correlated (fc). Core–valence electron correlation effects were investigated at the MP2 level correlating all electrons (ae) and using the correlation consistent polarized *weighted* core–valence basis sets (cc-pwCVnZ, n = D,T)[88] for carbon (C) and oxygen (O), as well as the cc-pwCVDZ-X2C and cc-pwCVTZ-X2C basis sets[89] for cerium (Ce). The corresponding optimized auxiliary basis sets[86,90] were also employed constructing those for cerium based on the procedure reported in Ref. 86. For consistency, the "def2" ECP for cerium has also been utilized. For the point charge embedding, the automated periodic electrostatic embedding method (PEECM)[24] was employed. In this method, the embedding is divided into two parts, the near-field (NF) and the far-field (FF). All the NF electrostatic interactions between the QM cluster and the point charge field are calculated by direct integration, while the rest of the interactions (FF) are computed by employing a multipole expansion of the Coulomb interactions[91–93] by the periodic fast multipole method.[94–96] To avoid polarization effects in the surroundings between the QM cluster and the point charges, a boundary region was defined where the positive point charges closer to the QM cluster, i.e., points with Ce^{4+}, were represented with the electrostatic core potential (ECP) ecp-18-mhf[97] for Ti^{4+} ions. This choice is based on the fact that the formal charge and the ionic radius of Ti^{4+} are similar to those of Ce^{4+}. All clusters were integrated into a charge field (+4 for Ce and −2 for O), which emulate the Madelung potential.[98] Within the embedded cluster model, the harmonic frequency of CO was numerically computed from analytic gradients in the case of MP2 calculations. For the CCSD(T) computations, the CO vibrational frequency was estimated from a HF-Hessian obtained from analytical gradients with correlation contributions estimated by dint of double numerical differentiation of energy points using central differences of gradients obtained by central differences, which results in $(6N)^2$ energy points (being N the number of atoms) applying displacements of 0.002 a_0. The accuracy of the numerical procedure was verified with the analytical procedure at the MP2 level, obtaining an agreement better than 1 cm^{-1}. For the gas phase calculations of CO, the correlation-consistent basis sets (cc-pVXZ)[99] were also employed using analytical second derivatives[100] as implemented in the quantum-chemical package CFOUR.[101] The anharmonic contribution to the potential energy was evaluated by numerical integration employing a Gauss–Hermite quadrature and reaching convergence with 13 grid points.[102]

III. RESULTS AND DISCUSSION

A. Analysis of the size of the QM cluster

Within the embedded cluster model, the first point to take into account is the definition of the quantum-mechanical cluster (QM) that is necessary and sufficient to describe the micro-kinetic or thermodynamic processes under study and which, at the same time, makes quantum chemical methods such as CCSD(T) accessible. For this purpose, four clusters were designed, i.e., cluster 1 $[CeO_7Ti_{12}]^{38+}$; cluster 2 $[Ce_4O_{22}Ti_{21}]^{56+}$; cluster 3 $[Ce_7O_{31}Ti_{24}]^{62+}$; and cluster 4 $[Ce_{10}O_{40}Ti_{33}]^{92+}$ (see Fig. 1). In Fig. 1, the boundary regions defined with ECPs of Ti^{4+} (blue color) were also included. This set of clusters was chosen such that the influence on the prediction of the CO stretching frequency due to the size and number of layers defined in the embedded cluster could be assessed. For this goal, the fc-MP2 method and three different basis sets, i.e., def2-SVP, def2-TZVPP, and def2-QZVPP, were used. To carry out the geometry optimizations, the surface structures were based on the periodic DFT results and kept fixed; only the structure of the CO molecule positioned perpendicular to the surface and aligned with the central Ce atom or the CO molecule and the aforementioned Ce atom were relaxed. The reason for this decision was based on previous evidence, which indicated that the most stable non-polar CeO_2(111) surface

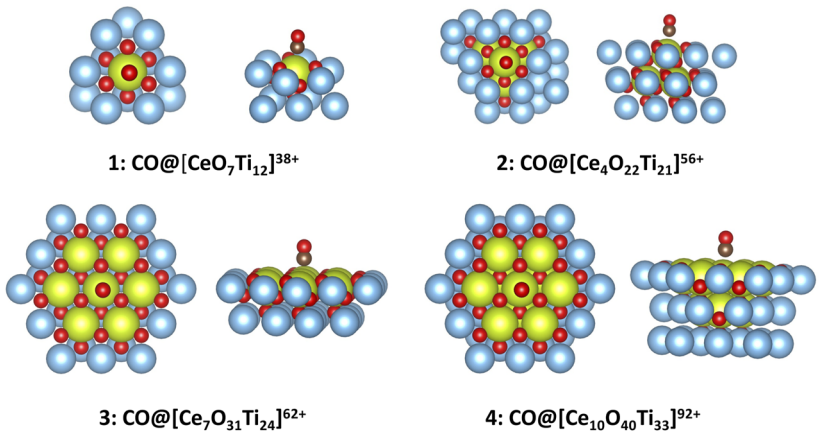

FIG. 1. Structure of the four clusters studied in this work: cluster 1: $[CeO_7Ti_{12}]^{38+}$; cluster 2: $[Ce_4O_{22}Ti_{21}]^{56+}$; cluster 3: $[Ce_7O_{31}Ti_{24}]^{62+}$; and cluster 4: $[Ce_{10}O_{40}Ti_{33}]^{92+}$. In all cases, the CO molecule is positioned perpendicular to the surface and aligns with the central Ce. (Cerium: green; titanium: blue; oxygen: red.)

experiences little relaxation effects with interlayer spacing changing by 0.02 Å at the most.[45,103–105] Furthermore, it should be noted that these clusters describe the case of low coverage, which must be taken into account when comparing with experimental data.

As it can be seen in Fig. 2, where data obtained with the def2-TZVPP basis set are displayed using surface structures obtained with three different functionals, i.e., BEEF-vdW, PBE-U(2 × 2), and HSE06(2 × 2), the effect of relaxing the geometry of the CO molecule

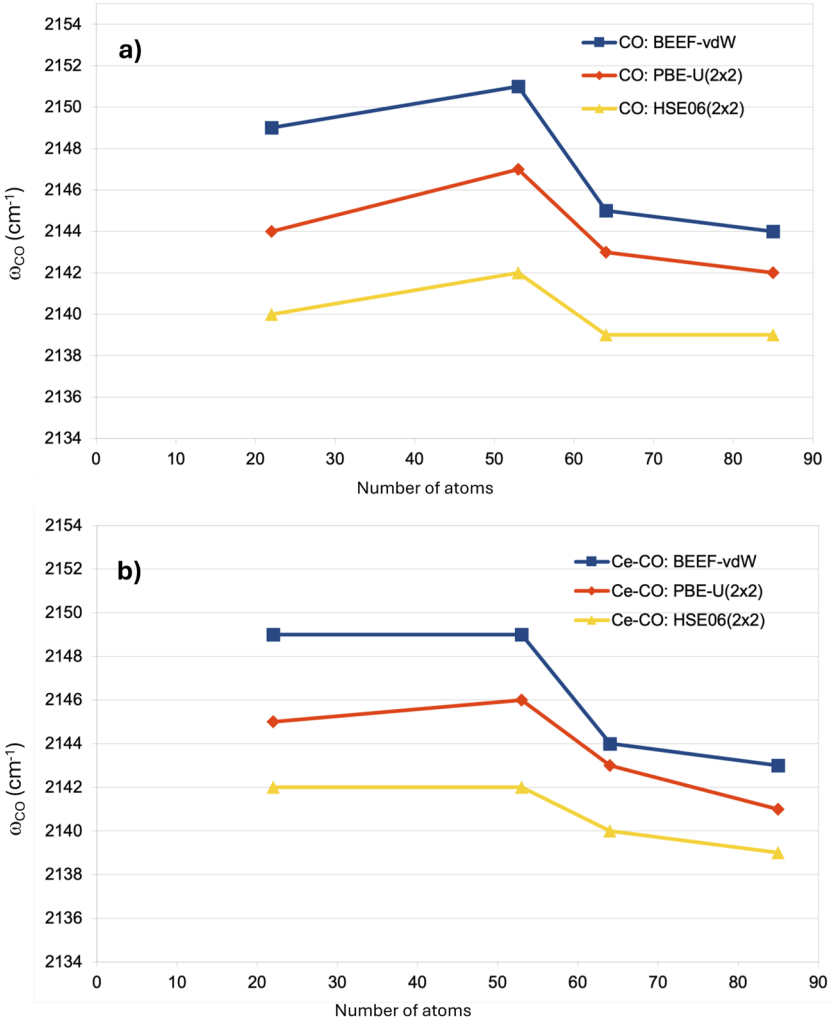

FIG. 2. fc-MP2/def2-TZVPP CO harmonic vibrational frequency. Cluster size and shape dependence analysis considering only the relaxation of CO (a) and that of CO–Ce (b). Results for cluster 1: $[CO@CeO_7Ti_{12}]^{38+}$; cluster 2: $[CO@Ce_4O_{22}Ti_{21}]^{56+}$; cluster 3: $[CO@Ce_7O_{31}Ti_{24}]^{62+}$; cluster 4: $[CO@Ce_{10}O_{40}Ti_{33}]^{92+}$ are displayed for surfaces obtained using the BEEF-vdW, PBE-U, and HSE06 functionals.

compared to that of CO–Ce represents differences in the prediction of the CO stretching frequency of at most 2 cm^{-1}. In addition, when analyzing the influence of the cluster size, it is observed that with clusters 3 and 4, the frequencies are essentially converged and that the values obtained with cluster 1 overestimate the harmonic vibrational frequency of CO by only 4 cm^{-1} in the worst case. For the surface structures obtained using the HSE06 hybrid functional, the dependence with respect to the cluster-size is also smaller. Similar conclusions can be drawn starting from other surfaces and using larger basis sets (see the supplementary material).

The relationship between cluster-size and basis-set size is shown representatively for the HSE06(2 × 2) surface using the MP2 method and three different basis sets in Fig. 3. (For the remaining surfaces, the results are similar and are provided in the supplementary material.) The trend observed is independent whether only the structure of the CO molecule adsorbed on the surface [Fig. 3(a)] or that of the CO–Ce group [Fig. 3(b)] is relaxed. The influence of the cluster size is much more relevant with the def2-SVP basis set for which differences between cluster 1 and cluster 4 of 10 cm^{-1} [Fig. 3(a)] and 6 cm^{-1} [Fig. 3(b)] are observed. In the case of the def2-TZVPP basis set, the cluster-size influence is much smaller with only differences of 2 and 4 cm^{-1} in the cases of relaxing only CO and CO–Ce, respectively. With an even larger basis set (def2-QZVPP) and although no data are available for cluster 4, it can be concluded that the difference between cluster 1 and larger clusters should not amount to higher than 2–4 cm^{-1}. In general, the use of the small def2-SVP basis set leads to misleading results.

B. CO vibrational frequency of $CO@CeO_2(111)$

The predictions of the harmonic vibrational frequency of CO on the $CeO_2(111)$ surface using the CCSD(T) method were carried

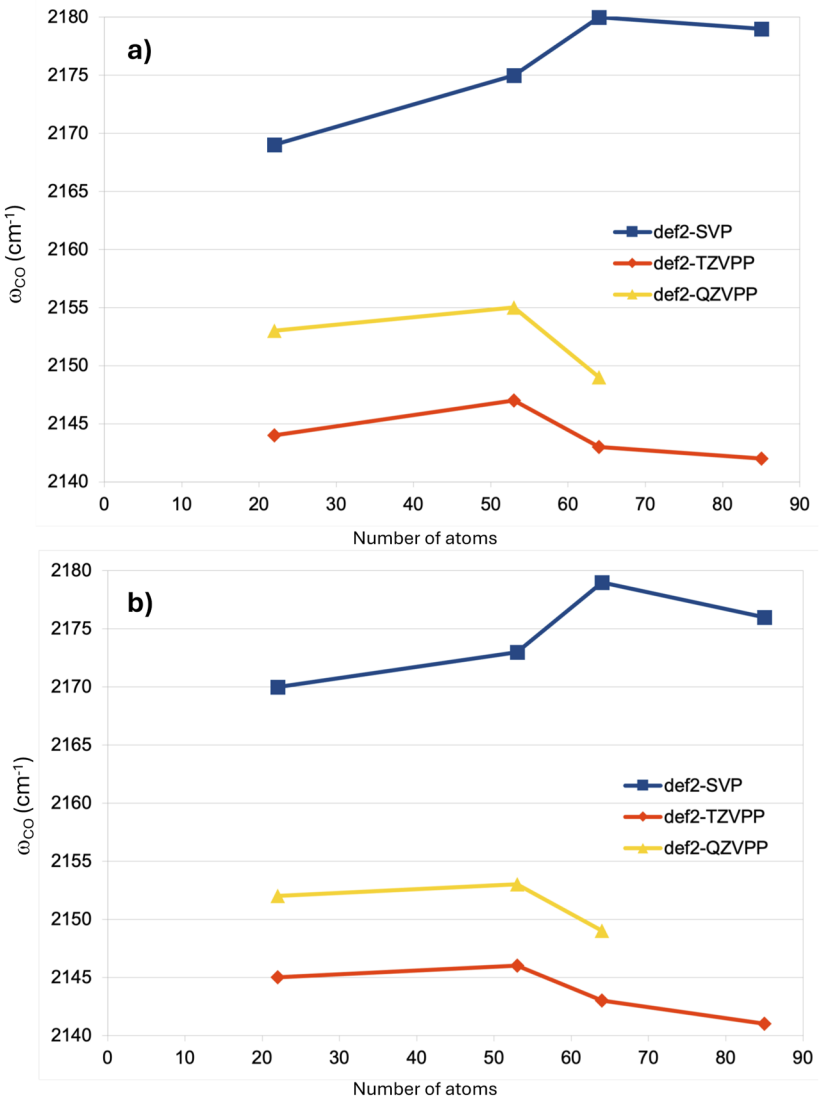

FIG. 3. fc-MP2 CO harmonic vibrational frequency. Cluster-size vs basis-set size analysis considering only the relaxation of the CO structure (a) and that of the CO–Ce trinomial (b). Results for cluster 1: $[CO@CeO_7Ti_{12}]^{38+}$; cluster 2: $[CO@Ce_4O_{22}Ti_{21}]^{56+}$; cluster 3: $[CO@Ce_7O_{31}Ti_{24}]^{62+}$; cluster 4: $[CO@Ce_{10}O_{40}Ti_{33}]^{92+}$ obtained employing the HSE06(2 × 2) surface.

out for cluster 1. In accordance with the results obtained with the MP2 method, an overestimation of 2–4 cm^{-1} is expected for this cluster size (see Sec. III A). Table I summarizes the values obtained with the MP2 and CCSD(T) methods for the five optimized $CeO_2(111)$ surfaces tested in this work. According to the results presented in Table I, the following points can be highlighted. First, analyzing the results with the PBE-U and HSE06 surfaces, it is concluded that the size of the unit cell is not relevant for the prediction of the vibrational frequency of CO. Second, in all cases and regardless of the basis set used, the value of the CO frequency predicted employing the PBE-U and HSE06 surfaces decreases by 3 and 14 cm^{-1}, respectively, in comparison with the values obtained with the BEEF-vdW surface. Comparing the performance of the MP2 method with the results obtained using CCSD(T), it is found that MP2 systematically underestimates the harmonic CO frequency by about 40–45 cm^{-1}. An overall assessment of the contribution of electron correlation is determined by comparing the data obtained with the HF method and those obtained with the CCSD(T) method. According to the data presented in Table S1 (supplementary material), the contribution of including electron correlation represents a reduction in the CO harmonic frequency of 258–360 cm^{-1}.

Turning now the attention to the basis set convergence of the computed harmonic frequencies, when going from def2-SVP to def2-TZVPP, the frequency decreases in the order of 26 and 20 cm^{-1} with the MP2 and CCSD(T) methods, respectively. In contrast, going from def2-TZVPP to def2-QZVPP, the frequency increases by 8 and 11 cm^{-1} with the MP2 and CCSD(T) methods, respectively. At this point, it is to be questioned if this trend is exclusive to these clusters and to what extend it depends on the use of the Karlsruhe basis sets. To clarify these issues, the values of the CO harmonic frequency for the free CO molecule obtained with the Karlsruhe basis sets (def2-SVP, def2-TZVPP, and def2-QZVPP) were analyzed in comparison with those obtained with the correlation-consistent basis sets (cc-pVXZ)[99] (see Table II). While with the cc-pVXZ hierarchy the harmonic frequency increases consistently by 10 cm^{-1} when going from cc-pVDZ to cc-pVTZ and from the latter to cc-pVQZ, an irregularity in the Karlsruhe def2-SVP basis set is observed, which overestimates the frequency by about 50 cm^{-1} in comparison with the cc-pVDZ and the def2-TZVPP basis sets. Regarding the polarized TZ- and QZ-quality basis sets, both hierarchies follow the same trend and result in similar values. Moreover, based on the value obtained with the cc-pV5Z basis set (see Table II), it can be concluded that both hierarchies reach convergence using the def2-QZVPP or cc-pVQZ basis sets. Comparing the experimental value of the CO harmonic frequency, i.e., 2169.756 cm^{-1},[106] with the theoretical predictions, it is revealed an underestimation for the CO frequency by about 42 and 6 cm^{-1} with the MP2 and CCSD(T) methods, respectively. In the latter case, this difference can be significantly reduced to −0.4 cm^{-1} by the inclusion of relativistic effects, core–valence corrections, and higher-order corrections to the coupled-cluster expansion.[107] From this analysis, it can be concluded that the results obtained for the $CO@[CeO_7Ti_{12}]^{38+}$ cluster follow the same behavior as observed in the CO molecule. This means that, first, that the results of the def2-SVP basis function are questionable when using wavefunction-based methods such as MP2 and CCSD(T) and, second, that the results obtained with the def2-QZVPP basis set can be considered converged with an underestimation of ~5 cm^{-1} due to the neglect of contributions such as relativistic effects, core–valence corrections, and higher-order coupled-cluster corrections.

With the goal of investigating some of the latter mentioned aspects, the influence of including diffuse basis functions and the effects of the core–valence correlation were additionally examined. MP2 calculations for cluster 1 using the optimized HSE06(1 × 1) surface were used as a model employing the def2-SVPD, def2-TZVPPD, def2-TZ/QZVPPD, and def2-QZVPPD basis sets as well as the cc-pwCV(D,T)Z-[Ce:X2C] basis sets. According to the results presented in Table S2 (see the supplementary material), adding diffuse functions has negligible effects, i.e., 1, −1, 4, and 2 cm^{-1} for def2-SVPD, def2-TZVPPD, def2-TZ/QZVPPD, and def2-QZVPPD, respectively, for the vibrational frequency of CO adsorbed on $CeO_2(111)$. The harmonic frequencies of CO(gas) are affected somewhat more by −29, −6, −1, and −1 cm^{-1}, indicating that def2-TZ/QZVPPD and def2-QZVPPD are sufficiently close to the basis set limit. Employing the cc-pwCVDZ/cc-pwCVDZ-X2C basis set described in Sec. II B, the core–valence correction (ae-fc) effects for cluster 1 [HSE06(1 × 1)] amount to 5 and 3 cm^{-1} for

TABLE I. Harmonic CO stretching frequency (in cm^{-1} units) for cluster 1 $CO@[CeO_7Ti_{12}]^{38+}$ obtained for the five different optimized $CeO_2(111)$ surfaces tested in this work.[a,b]

Method	Basis set	Functional and unit cell size used by the surface optimization				
		BEEF-vdW	PBE-U(1 × 1)	PBE-U(2 × 2)	HSE06(1 × 1)	HSE06(2 × 2)
fc-MP2	def2-SVP	2172	2170	2170	2166	2166
	def2-TZVPP	2147	2144	2144	2140	2140
	def2-TZ/QZVPP	2155	2152	2152	2148	2148
	def2-QZVPP	2155	2153	2153	2148	2148
fc-CCSD(T)	def2-SVP	2207	2204	2204	2200	2200
	def2-TZVPP	2187	2184	2184	2179	2179
	def2-TZ/QZVPP	2199	2196	2196	2190	2190

[a]Masses of 12.000 000 u and 15.994 914 630 u for C and O, respectively, were used in all cases.
[b]The designation def2-TZ/QZVPP refers to the use of the def2-QZVPP basis set for CO and the Ce atom directly interacting with the CO molecule and of the def2-TZVPP basis set for the rest of the QM cluster.

TABLE II. Harmonic frequency of CO(gas) (in cm^{-1}) calculated using the MP2 and CCSD(T) methods and employing different basis sets.[a]

Method	Basis set		Basis set	
fc-MP2	def2-SVP	2172	cc-pVDZ	2114
	def2-TZVPP	2122	cc-pVTZ	2121
	def2-QZVPP	2127	cc-pVQZ	2128
			cc-pV5Z	2127
fc-CCSD(T)	def2-SVP	2202	cc-pVDZ	2143
	def2-TZVPP	2155	cc-pVTZ	2153
	def2-QZVPP	2163	cc-pVQZ	2164
			cc-pV5Z	2164

[a]Masses of 12.000 000 u and 15.994 914 630 u for C and O, respectively, were used in all cases.

the cluster 1 model and $CO_{(gas)}$, respectively. However, using the cc-pwCVTZ/cc-pwCTZ-X2C basis set, values of 9 and 9 cm^{-1} are obtained, for cluster 1 and $CO_{(gas)}$, respectively. This is quantitatively equivalent to the accurate gas-phase value of Ref. 107 and also indicates that the frequency shift between cluster and gas-phase is not affected by the core–valence correlation.

In order to bring the theoretical predictions closer to the experimental observation, the harmonic vibrational frequencies were corrected for the effects of anharmonicity. In the present work, the anharmonic contribution was directly evaluated by employing an approach that combines a Finite Basis Representation (FBR) with a Discrete Variable Representation (DVR) of the potential energy based on vibrational normal coordinates and in conjunction with an analytic form of the kinetic energy operator.[102] This model was considered appropriate taking into account the weakly bound nature of CO as well as its relatively small anharmonic character. The approach applied in this investigation contrasts with the method-dependent factor[47,48] usually employed in theoretical catalysis, which consists of a scaling process based on the experimental and calculated frequencies of the CO molecule, i.e., $\lambda = \frac{\nu^{exp}_{CO_{gas}}}{\nu^{cal}_{CO_{gas}}}$ with $\nu^{exp}_{CO_{gas}}$ = 2143 cm^{-1} and where λ is the scale factor by which the harmonic frequency calculated for CO adsorbed on the surface is to be multiplied. The values obtained in this research are presented in Table III. The anharmonic corrections amount to about 24–25 cm^{-1} regardless of method and basis set used. This small dependence of methods and basis set has been previously observed for gas phase molecules; see, for example, the pioneering work of Handy *et al.*[110] in this regard. Furthermore, this value is in complete agreement with the experimental anharmonicity of the CO molecule (26.5716 cm^{-1})[106] and confirms the weakly bound character of CO on the CeO_2(111) surface. At the same time, this result explains why the method-dependent factor performs very well for this case[48] since the scale factor accounts only for the different performance of the theoretical method (i.e., the periodic DFT functional) when considering the molecule in the gas phase or adsorbed on the surface. Moreover, the evaluation of the results presented in Table III indicates that the functional used in the optimization of the surface plays a relevant role, when comparing with the experimental value. Therefore, and according to the criteria discussed above, it is reasonable to state that the best prediction of the CO frequency on the CeO_2(111) surface is obtained with the CCSD(T)/def2-TZ/QZVPP method using the HSE06 surface. This represents a difference from the experimental data of 12 cm^{-1}, which is plausible considering the error of approximately +4 cm^{-1} resulting from considering a low coverage ($\theta \approx \frac{1}{4}$), which is the case under the embedding cluster model here defined, and according to the analysis reported in the most recent periodic DFT studies.[48] In other words, it would be an experimental blue shift of ≈4 cm^{-1} in the case of low coverage, which represents a difference of ≈8 cm^{-1} with the theoretical prediction presented in this work. This phenomenon has been previously observed for CO adsorbed on MgO(001), where depending of the surface coverage, there is a single band shifting from 2157.5 cm^{-1} (at $\theta \rightarrow 0$) to 2150.2 cm^{-1} (at $\theta = \frac{1}{4}$).[111] In contrast with the results presented here, a recent study using periodic LNO-CCSD(T)[112]

TABLE III. Computed anharmonic CO stretching frequency (in cm^{-1}) for the cluster $CO@[CeO_7Ti_{12}]^{38+}$ obtained for the five different optimized surfaces tested in this work. The data in parentheses and italic correspond to the anharmonic correction (in cm^{-1}).[a,b]

		Functional and cell size used for the surface optimization					
Method	Basis set	BEEF-vdW	PBE-U(1 × 1)	PBE-U(2 × 2)	HSE06(1 × 1)	HSE06(2 × 2)	Exp.[c]
fc-MP2	def2-SVP	2148 *(−24)*	2145 *(−24)*	2145 *(−24)*	2142 *(−24)*	2142 *(−24)*	2154
	def2-TZVPP	2122 *(−25)*	2120 *(−25)*	2120 *(−25)*	2115 *(−25)*	2115 *(−25)*	
	def2-TZ/QZVPP	2130 *(−25)*	2127 *(−25)*	2127 *(−25)*	2123 *(−25)*	2123 *(−25)*	
	def2-QZVPP	2130 *(−25)*	2128 *(−25)*	2128 *(−25)*	2123 *(−25)*	2123 *(−25)*	
fc-CCSD(T)	def2-SVP	2182 *(−24)*	2179 *(−24)*	2179 *(−24)*	2176 *(−25)*	2176 *(−25)*	
	def2-TZVPP	2163 *(−25)*	2159 *(−25)*	2159 *(−25)*	2154 *(−25)*	2154 *(−25)*	
	def2-TZ/QZVPP	2174 *(−24)*	2171 *(−25)*	2171 *(−25)*	2166 *(−25)*	2166 *(−25)*	

[a]Masses of 12.000 000 u and 15.994 914 630 u for C and O, respectively, were used in all cases.
[b]The designation def2-TZ/QZVPP refers to the use of the def2-QZVPP basis set for CO and the Ce atom directly interacting with the CO molecule and of the def2-TZVPP basis set for the rest of the QM cluster.
[c]Polarization-resolved IRRAS experiment of 1 monolayer (ML) CO adsorbed on oxidized CeO_2(111) single crystal surfaces at a low temperature (75 K).[108,109]

predicts the CO vibrational frequency on CO@MgO(001) ($\theta \rightarrow 0$) at 2173.9 cm^{-1}, which is 16.4 cm^{-1} larger than the experimental value.[111]

Added to this, it is needed to bear in mind the experimental error of the IRRAS (Infrared Reflection Adsorption Spectroscopy) experiments where different experimental values could exist, as the spectra are not always recorded under the same conditions and it is often assumed that the surfaces are completely perfect (e.g., no defects and low CO coverage). When IRRAS data for model systems, such as probe molecules adsorbed to single crystals, are available, one could expect an uncertainty of ~±2–4 cm^{-1}.[34,37] For all this, in many cases, instead of analyzing absolute frequency values, it is more coherent either to analyze the frequency shift of characteristic frequencies of the molecule adsorbed on different surfaces [e.g., $CeO_2(111)$ and $CeO_2(110)$] or frequency shift of characteristic frequencies of the molecule adsorbed on a surface in relation to those of the molecule in the gas phase. In the latter case, the experimental results indicate a blue shift of 11 cm^{-1} of the frequency of CO adsorbed in $CeO_2(111)$ [1 monolayer (ML) coverage] compared to $CO_{(gas)}$. The predictions made in the present work indicate a theoretical blue shift of 29 cm^{-1} (CCSD(T)/def2-TZ/QZVPP) ($\theta \approx \frac{1}{4}$ coverage), which represents a clear overestimation in comparison with the experimental shift (+11 cm^{-1}). This can be partially explained by considering the intrinsic error due to the use of cluster 1 (an overestimation of ~4 cm^{-1}; see Sec. III A) and the fact that the embedded cluster model presented here addresses only the low-coverage case, which according to previous studies[48] means an additional overestimation of about 4 cm^{-1}. Taking these two factors into account, the $\nu_{CO_{(ads)}} - \nu_{CO_{(gas)}}$ is ~21 cm^{-1}. In addition, aspects such as the non-inclusion of relativistic effects, core–valence corrections, as well as higher-orders in the coupled-cluster expansion play different quantitative roles in the CO vibrational frequency in the gas phase [underestimated by 6 cm^{-1} at the CCSD(T)/def2-QZVPP level of theory] and adsorbed on $CeO_2(111)$ (overestimated by 7 cm^{-1}). This scenario again differs from the vibrational frequency shift obtained for CO adsorbed on MgO(001) in which making use of periodic LNO-CCSD(T), both the CO vibrational frequency in the gas phase and adsorbed on MgO were equally overestimated by 16 cm^{-1}. This is why the theoretical frequency shift of +14.7 cm^{-1} is in excellent agreement with the experimental shift of +14.3 cm^{-1}.[112]

C. CO binding energy to the $CeO_2(111)$ surface

The adsorption energy of CO adsorbed on the $CeO_2(111)$ surface was calculated according to the following formula:

$$E_{ads} = E[CO@CeO_2(111)] - E[CeO_2(111)] - E[CO_{gas}], \quad (1)$$

where $E[CO@CeO_2(111)]$, $E[CeO_2]$, and $E[CO_{(gas)}]$ represent the surface energy with the adsorbed CO molecule (i.e., one of the embedded clusters; see Fig. 1), the surface energy without adsorbate (i.e., embedded clusters without CO adsorbed), and the energy of the CO molecule, respectively. This expression for the adsorption energy was approximately corrected for the basis-set superposition error (BSSE) employing the full counterpoise (CP)[113] scheme. This means that the molecule-surface adsorption energy was actually defined as

$$E_{int} = E[CO@CeO_2(111)] - \tilde{E}[CeO_2(111) + \text{ghosts}] - \tilde{E}[CO_{(gas)} + \text{ghosts}], \quad (2)$$

where $\tilde{E}[CeO_2(111) + \text{ghosts}]$ and $\tilde{E}[CO_{(gas)} + \text{ghosts}]$ are the energies of the fragments at the same coordinates as in the embedded cluster with adsorbate (denoted as $[CeO_2(111)@CO]$) and employing the full system basis set, which means "ghost" basis for the missing fragment. To this correction, the adjustment due to the relaxation of the CO molecule as well as a contribution coming from the vibrational zero-point energy (ZPE) was also added. For the latter, only the 3N (N = 2) vibrational degrees of freedom of the CO molecule adsorbed on the surface and the 3N-5 vibrational degrees of freedom of the free CO molecule were considered. Values for cluster 1 ($CO@[CeO_7Ti_{12}]^{38+}$) and cluster 2 ($CO@[Ce_4O_{22}Ti_{21}]^{56+}$) with (wBSSE) and without (woBSSE) basis set superposition error correction are listed in Table IV.

The most recent results obtained with periodic DFT and for a low CO coverage ($\theta = \frac{1}{4}$) estimated the CO binding energy of −0.13 eV, while previous embedded cluster models using the method of increments[57–59] evaluated this magnitude to more than −0.25 eV.[51] In the latter case, single-point HF energies and single-point electron-correlation contributions obtained at MP2 and CCSD(T) methods with polarized TZ- and DZ-quality basis sets, respectively, were sequentially added to the energy of a structure optimized at the B3LYP/aug-cc-pVTZ level and the BSSE was only considered in the first term of the increment expansion. Keeping in mind the importance that electron correlation can play in a correct and consistent treatment of physisorption interactions, in the present work, the binding energy was evaluated in a different manner from the incremental scheme, that is, employing a single method [MP2 and CCSD(T)] in conjunction with a particular basis set (def2-SVP, def2-TZVPP, and def2-QZVPP). Regarding the counterpoise (CP) correction, it is recognized in the literature that the CP scheme is only an approximation[115,116] converging often at the complete basis set (CBS) limit. In fact, multiple studies had led to propose the use of only half of the CP correction, what has been recently called as a "*heuristic*" suggestion.[117] In keeping with this idea, the most reasonable value for the binding energy would be between the results with and without the BSSE correction. Having said that, the first conclusion drawn concerning the MP2 results is that the size of the cluster does not have a significant influence on the values obtained for the binding energy with a slight underestimation [(−0.03) eV–(−0.04) eV] for cluster 1 in comparison with cluster 2. Next, it is to be pointed out that the size of the supercell used for the periodic calculations, i.e., (1 × 1) and (2 × 2), has no influence on the binding energy as in the case for the CO stretching frequency. Third, the following trend is observed concerning the influence of the functionals used in periodic calculations over the magnitude of the binding energy: $|E_{ads}(\text{BEEF-vdW})| > |E_{ads}(\text{PBE-U})| > |E_{ads}(\text{HSE06})|$. For example, the binding energies obtained with the HSE06-surface structures are of the order of 0.04–0.05 eV smaller than those resulting from PBE-U-surface structures. Another aspect to comment on is the performance of the MP2 and CCSD(T) correlation methods. MP2 tends to slightly overestimate the binding energy compared to the results obtained with the CCSD(T) method, with values being ~0.03–0.04 eV larger. The latter trend is in line with the underestimation (redshift) of the harmonic frequency of

TABLE IV. CO adsorption energy (E_{ads} in eV) for cluster 1 ($CO@[CeO_7Ti_{12}]^{38+}$) and cluster 2 ($CO@[Ce_4O_{22}Ti_{21}]^{56+}$) obtained for the five different optimized CeO_2(111) surfaces tested in this work as well as calculated literature values ($E_{ads}^{lit.}$ in eV).[a,b,c,d]

		Functional and cell size used for the surface optimization										
		BEEF-vdW		PBE-U(1 × 1)		PBE-U(2 × 2)		HSE06(1 × 1)		HSE06(2 × 2)		
Method	Basis set	woBSSE	wBSSE	woBSSE	wBSSE	woBSSE	wBSSE	woBSSE	wBSSE	woBSSE	wBBSE	$E_{ads}^{lit.}$
Cluster 1: $CO@[CeO_7Ti_{12}]^{38+}$												
fc-MP2	def2-SVP	−0.41	+0.03	−0.38	+0.05	−0.38	+0.05	−0.32	+0.06	−0.32	+0.06	−0.26[e,f]
	def2-TZVPP	−0.38	−0.21	−0.34	−0.19	−0.34	−0.19	−0.30	−0.15	−0.30	−0.15	−0.28[g,h]
	def2-TZ/QZVPP	−0.43	−0.23	−0.40	−0.21	−0.40	−0.21	−0.35	−0.17	−0.35	−0.17	−0.27[f,i]
	def2-QZVPP	−0.38	−0.26	−0.35	−0.24	−0.35	−0.24	−0.30	−0.19	−0.30	−0.19	
fc-CCSD(T)	def2-SVP	−0.38	+0.06	−0.35	+0.07	−0.35	+0.07	−0.30	+0.08	−0.30	+0.08	−0.18[f,j]
	def2-TZVPP	−0.34	−0.18	−0.31	−0.16	−0.31	−0.16	−0.27	−0.12	−0.27	−0.12	−0.13[f,k]
	def2-TZ/QZVPP	−0.39	−0.19	−0.36	−0.17	−0.36	−0.17	−0.32	−0.14	−0.32	−0.14	
Cluster 2: $CO@[Ce_4O_{22}Ti_{21}]^{56+}$												
fc-MP2	def2-SVP	−0.44	+0.01	−0.41	+0.03	−0.42	+0.03	−0.36	+0.05	−0.36	+0.05	
	def2-TZVPP	−0.41	−0.23	−0.38	−0.21	−0.38	−0.21	−0.33	−0.17	−0.33	−0.17	
	def2-TZ/QZVPP	−0.47	−0.25	−0.45	−0.23	−0.45	−0.23	−0.41	−0.19	−0.41	−0.19	
	def2-QZVPP	−0.41	−0.28	−0.38	−0.25	−0.38	−0.25	−0.34	−0.21	−0.34	−0.21	

[a] *woBSSE*: without basis set superposition error (BSSE) correction. *wBSSE*: with BSSE correction.
[b] BSSE includes four contributions: the binding energy; second, Counterpoise (CP) corrections of the basis-set superposition error (BSSE) (see text); the relaxation of the CO structure; and finally the part corresponding to the harmonic vibrational zero-point energy of CO (ZPE) (see text).
[c] Masses of 12.000 000 u and 15.994 914 630 u for C and O, respectively, were used in all cases.
[d] The designation def2-TZ/QZVPP refers to using the def2-QZVPP basis set for CO and the Ce atom directly interacting with the CO molecule and the def2-TZVPP basis set for the rest of the QM cluster.
[e] Reference 114.
[f] Denotes theoretical estimates using DFT under periodic boundary conditions.
[g] Reference 51.
[h] Denotes computations using an embedded cluster model[14] in conjunction with the method of increments[57–59] to assess the binding energy.
[i] References 108 and 109.
[j] Reference 48. Periodic DFT using the PBE functional together with a Hubbard U-like term.
[k] Reference 48. Periodic DFT using the hybrid functional HSE06 and $\theta = \frac{1}{4}$ CO coverage.

CO observed with the MP2 method in comparison with the experimental value of $CO_{(gas)}$ as well as to the predictions obtained with the CCSD(T) method (see Sec. III B). These results indicate that the influence of the employed surfaces is greater than that obtained by improving the electron correlation treatment.

The use of additional diffuse functions for cluster 1 using the optimized HSE06(1 × 1)-surface and computed at the MP2 level has larger effects on the adsorption energies. All adsorption energies become more negative, i.e., −0.08 eV (def2-TZVPPD), −0.05 eV (def2-TZ/QZVPPD), and −0.03 eV (def2-QZVPPD) for the adsorption energies without CP correction and 0.04 eV (def2-TZVPPD, −0.03 (def2-TZ/QZVPPD), and −0.02 eV (def2-QZVPPD) for the adsorption energies with CP correction. While the changes for the larger basis sets are noticeable, they are only 8%–15% for the two larger basis sets considered in the present study and therefore negligible within the expected accuracy of the current approach. Changes from −0.17 to −0.20 eV or −0.19 to −0.21 eV as observed here do not alter the qualitative interpretation of the adsorption energies. At the MP2/cc-pwCVDZ level, the core–valence correction amounts to −0.02 and 0.00 eV for cluster 1 [HSE06 (1 × 1)] or the adsorption energies with/without CP correction, respectively. With cc-pwCVTZ, the results change to −0.02 and −0.01 eV; this indicates that core–valence corrections are negligible for adsorption energies determined in this study. To conclude and assuming the superior performance of the screened range-separated hybrid functional HSE06,[118,119] it is proposed as the best estimate for the CO binding energy of a value between −0.32 eV (woBSSE) and −0.13 eV (wBSSE), i.e., −0.22 ± 0.07 eV obtained with the CCSD(T)/def2-TZ/QZVPP method. This proposed value is in between the results obtained using periodic DFT employing the hybrid functional HSE06[48] (−0.13 eV) and those obtained previously using the incremental method[51] (−0.28 eV).

IV. CONCLUSIONS

This work presents a scheme to apply accurate methods such as CCSD(T), to investigate the adsorption of molecules on surfaces choosing the probe molecule CO adsorbed on the non-polar

$CeO_2(111)$ facet as an example. The reported course of action combines surface structure optimizations using periodic DFT with affordable wavefunction based methods such as CCSD(T) and large basis sets (e.g., polarized TZ- and QZ-quality) within the framework of embedding cluster model PEECM. The suggested protocol offers a way to predict the vibrational spectroscopic features of molecules adsorbed on surfaces with a quantitative level of accuracy. Based on the results of this research, the following conclusions can be made:

- The periodic DFT estimates to determine the best surface structure play a significant role to achieve an acceptable level of accuracy. It is found that hybrid functionals such as HSE06 perform superiorly than van der Waals functionals (BEEF-vdW) and GGA functionals in conjunction with a Hubbard U-like term (PBE + U) with values for the CO frequency closer to the experimental data and binding energies more in line with weakly bound systems.
- For low-coverage cases, the supercell size used by the periodic DFT optimization is irrelevant for predicting the CO vibrational frequency and its binding energy.
- In the case of working with rare earth oxide surfaces, it is a reasonable approach to keep the best optimized structure using periodic DFT fixed and optimize only the structure of the molecule and the surface atoms directly linked to the adsorbed molecule within the embedded cluster model.
- Equally related to the type of surface, i.e., a rare earth oxide, the size and shape of the QM cluster (i.e., dimension of the first and second surface layers and the number of total cluster layers) could result in errors of $\sim\pm 2$–$4\ cm^{-1}$. This fact has made possible the accessibility of methods such as CCSD(T) with polarized triple or quadruple zeta basis sets, resulting in an error of $\sim\pm 5\ cm^{-1}$.
- The MP2 method independently of the basis set used underestimates the CO vibrational frequency by about 40–45 cm^{-1} in comparison with experiment and using the def2-QZVPP basis set.
- Considering the above-mentioned theoretical and computational errors and assuming an experimental uncertainty of about 2–4 cm^1 (adsorption on single crystals), our best estimate for the CO stretching is $2166 \pm 5\ cm^{-1}$ obtained at the CCSD(T)/def2-TZ/QZVPP level and employing a surface optimized with the HSE06 functional.
- With the procedure presented here, the determination of the $CO@CeO_2(111)$ adsorption energy happens to be a more difficult task. Different contributions playing "all" a decisive role to the binding energy make an accurate estimate challenging. In this context, just to mention the strong influence of the DFT functional used for surface optimization, the contribution coming from electron correlation treated by MP2 vs CCSD(T), and the approximate nature of the BSSE correction altogether lead to suggest only a conservative best estimate of about −0.22 eV, with an uncertainty error of about ±0.07 eV.

In summary, this work represents a first step to bring correlation methods to surface vibrational spectroscopy. For this purpose, the CO stretching frequency on the $CeO_2(111)$ surface was benchmarked. This research establishes a protocol, which can be applied to other low-index CeO_2 surfaces, with and without the presence of oxygen vacancies and to cases such as methane oxidation, where the absorbate interaction with the surface is rather weak and highly accurate calculations could be decisive to interpret the experimental results.

SUPPLEMENTARY MATERIAL

The supplementary material contains detailed information on the effects of cluster size when using surfaces optimized with different functionals and supercell sizes as well as employing diverse basis sets in the post-Hartree–Fock calculations.

ACKNOWLEDGMENTS

This work was funded by the German Research Foundation [Deutsche Forschungsgemeinschaft (DFG)] – SFB 1441–Project-ID 426888090 (projects A4 and B4). The authors acknowledge the support by the state of Baden-Württemberg bwHPC and the German Research Foundation (DFG) through Grant No. INST 40/575-1 FUGG (JUSTUS 2 cluster).

AUTHOR DECLARATIONS

Conflict of Interest

The authors have no conflicts to disclose.

Author Contributions

Juana Vázquez Quesada: Conceptualization (lead); Data curation (lead); Formal analysis (lead); Investigation (lead); Methodology (lead); Software (lead); Validation (lead); Visualization (lead); Writing – original draft (lead); Writing – review & editing (lead). **Sarah Bernart**: Investigation (supporting); Writing – review & editing (supporting). **Felix Studt**: Funding acquisition (equal); Writing – review & editing (supporting). **Yuemin Wang**: Formal analysis (supporting); Funding acquisition (equal); Writing – review & editing (supporting). **Karin Fink**: Funding acquisition (equal); Methodology (equal); Writing – review & editing (equal).

DATA AVAILABILITY

The data that support the findings of this study are available within the article and its supplementary material.

REFERENCES

[1] P. Huang and E. A. Carter, "Advances in correlated electronic structure methods for solids, surfaces, and nanostructures," Annu. Rev. Phys. Chem. **59**, 261 (2008).
[2] P. Huang and E. A. Carter, "Self-consistent embedding theory for locally correlated configuration interaction wave functions in condensed matter," J. Chem. Phys. **125**, 084102 (2006).
[3] X. Wen, J.-N. Boyn, J. M. P. Martinez, Q. Zhao, and E. A. Carter, "Strategies to obtain reliable energy landscapes from embedded multireference correlated wavefunction methods for surface reaction," J. Chem. Theory Comput. **20**, 6037 (2024).
[4] C. Sheldon, J. Paier, D. Usvyat, and J. Sauer, "Hybrid RPA:DFT approach for adsorption on transition metal surfaces: Methane and ethane on platinum (111)," J. Chem. Theory Comput. **20**, 2219 (2024).
[5] T. Schäfer, A. Gallo, A. Irmler, F. Hummel, and A. Grüneis, "Surface science using coupled cluster theory via local Wannier functions and in-RPA-embedding: The case of water on graphitic carbon nitride," J. Chem. Phys. **155**, 244103 (2021).

[6]T. Schäfer, F. Libisch, G. Kresse, and A. Grüneis, "Local embedding of coupled cluster theory into the random phase approximation using plane waves," J. Chem. Phys. **154**, 011101 (2021).
[7]H.-H. Lin, L. Maschio, D. Kats, D. Usvyat, and T. Heine, "Fragment-based restricted active space configuration interaction with second-order corrections embedded in periodic Hartree–Fock wave function," J. Chem. Theory Comput. **16**, 7100 (2020).
[8]B. T. G. Lau, G. Knizia, and T. C. Berkelbach, "Regional embedding enables high-level quantum chemistry for surface science," J. Phys. Chem. Lett. **12**, 1104 (2021).
[9]H.-Z. Ye and T. C. Berkelbach, "Ab initio surface chemistry with chemical accuracy: Application to water on metal oxides," arXiv:2309.14640 (2024).
[10]H.-Z. Ye and T. C. Berkelbach, "Periodic local coupled-cluster theory for insulator and metals," J. Chem. Theory Comput. **20**, 8948 (2024).
[11]R. E. Watson, "Analytic Hartree-Fock solutions for $O^{=}$," Phys. Rev. **111**, 1108 (1958).
[12]J. Li, H. L. Liu, and J. Ladik, "Calculation of the electron distribution of the $YBa_2Cu_3O_7$ cluster using a SCF Madelung potential," Chem. Phys. Lett. **230**, 414 (1994).
[13]B. Herschend, M. Baudin, and K. Hemansson, "A combined molecular dynamics + quantum mechanics method for investigation of dynamics effects on local surface structures," J. Chem. Phys. **120**, 4939 (2004).
[14]C. Müller and K. Hermansson, "Assessment methods for embedding schemes—Ceria as an example," Surf. Sci. **603**, 3329 (2009).
[15]H. M. Evjen, "On the stability of certain heteropolar crystals," Phys. Rev. **39**, 675 (1932).
[16]L. Z. Stolarczyk and L. Piela, "Direct calculation of lattice sums. A method to account for the crystal field effects," Int. J. Quantum Chem. **22**, 911 (1982).
[17]L. Piela, J. L. Brédas, and J. M. André, "Cancellation of low order electric moments of the unit cell: An efficient way of calculating crystal field effects in Hartree-Fock computations on periodic systems," J. Chem. Phys. **78**, 295 (1983).
[18]A. Laio, J. VandeVondele, and U. Rothlisberger, "A Hamiltonian electrostatic coupling scheme for hybrid Car–Parrinello molecular dynamics simulations," J. Chem. Phys. **116**, 6941 (2002).
[19]K. Götz, F. Meier, C. Gatti, A. M. Burow, M. Sierka, J. Sauer, and M. Kaupp, "Modeling environmental effects on charge density distributions in polar organometallics: Validation of embedded cluster models for the methyl lithium crystal," J. Comput. Chem. **31**, 2568 (2010).
[20]A. Kubas, D. Berger, H. Oberhofer, D. Maganas, K. Reuter, and F. Neese, "Surface adsorption energetics studied with 'gold standard' wave-function-based ab initio methods: Small-molecule binding to TiO_2(110)," J. Phys. Chem. Lett. **7**, 4207 (2016).
[21]B. X. Shi, A. Zen, V. Kapil, P. R. Nagy, A. Michaelides, and A. Grüneis, "Many-body methods for surface chemistry come of age: Achieving consensus with experiments," J. Am. Chem. Soc. **145**, 25372 (2023).
[22]B. X. Shi, V. Kapil, A. Zen, J. Chen, A. Alavi, and A. Michaelides, "General embedded cluster protocol for accurate modeling of oxygen vacancies in metal-oxides," J. Chem. Phys. **156**, 124704 (2022).
[23]R. H. Lavroff, D. Kats, L. Maschio, N. Bogdanov, A. Alavi, A. N. Alexandrova, and D. Usvyat, "Aperiodic fragments in periodic solids: Eliminating the need for supercells and background charges in electronic structure calculations of defects," arXiv:2406.03373 (2024).
[24]A. M. Burow, M. Sierka, J. Döbler, and J. Sauer, "Point defects in CaF_2 and CeO_2 investigated by the electrostatic embedded cluster method," J. Chem. Phys. **130**, 174710 (2009).
[25]D. Stodt, H. Noei, C. Hättig, and Y. Wang, "A combined experimental and computational study on the adsorption and reactions of NO on ritile TiO_2," Phys. Chem. Chem. Phys. **15**, 466 (2013).
[26]A. Rushiti and C. Hättig, "Activation of molecular O_2 on $CoFe_2O_4$ (001) surfaces: An embedded cluster study," Chem.-Eur. J. **27**, 17115 (2021).
[27]Q. N. Tran, O. Gimello, N. Tanchoux, M. Ceretti, S. Albonetti, W. Paulus, B. Bonelli, and F. Di Renzo, "Transition metal B-site substitutions in $LaAlO_3$ perovskites reorient bio-ethanol conversion reactions," Catalysts **11**, 344 (2021).
[28]O. Padilla, J. Munera, J. Gallego, and A. Santamaria, "Approach to the characterization of monolithic catalysts based on la perovskite-like oxides and their application for VOC oxidation under simulated indoor environment conditions," Catalysts **12**, 168 (2022).
[29]J. Feng, X. Zhang, J. Wang, X. Ju, L. Liu, and P. Chen, "Applications of rare earth oxides in catalytic ammonia synthesis and decomposition," Catal. Sci. Technol. **11**, 6330 (2021).
[30]J. Paier, C. Penschke, and J. Sauer, "Oxygen defects and surface chemistry of ceria: Quantum chemical studies compared to experiment," Chem. Rev. **113**, 3949 (2013).
[31]T. Montini, M. Melchionna, M. Monai, and P. Fornasiero, "Fundamentals and catalytic applications of CeO_2-based materials," Chem. Rev. **116**, 5987 (2016).
[32]E. W. McFarland and H. Metiu, "Catalysis by doped oxides," Chem. Rev. **113**, 4391 (2013).
[33]W. Song, L. Chen, L. Wan, M. Jing, and Z. Li, "The influence of doping amount on the catalytic oxidation of formaldehyde by Mn-CeO_2 mixed oxide catalyst: A combination of DFT and microkinetic study," J. Hazard. Mater. **425**, 127985 (2022).
[34]C. Wöll, "Structure and chemical properties of oxide nanoparticles determined by surface-ligand IR spectroscopy," ACS Catal. **10**, 168 (2020).
[35]G. Pacchioni, "Quantum chemistry of oxide surfaces: From CO chemisorption to the identification of the structure and nature of point defects on MgO," Surf. Rev. Lett. **07**, 277 (2000).
[36]M. Xu, H. Noei, K. Fink, M. Muhler, Y. Wang, and C. Wöll, "The surface science approach for understanding reactions on oxide powders: The importance of IR spectroscopy," Angew. Chem., Int. Ed. **51**, 4731 (2012).
[37]Y. Wang and C. Wöll, "IR spectroscopic investigations of chemical and photochemical reactions on metal oxides: Bridging the materials gap," Chem. Soc. Rev. **46**, 1875 (2017).
[38]C. Yang, M. Capdevila-Cortada, C. Dong, Y. Zhou, J. Wang, X. Yu, A. Nefedov, S. Heißler, N. López, W. Shen, Y. Wang, and C. Wöll, "Surface refaceting mechanism on cubic ceria," J. Phys. Chem. Lett. **11**, 7925 (2020).
[39]L. Caulfield, E. Sauter, H. Idriss, Y. Wang, and C. Wöll, "Bridging the pressure and materials gap in heterogeneous catalysis: A combined UHV, in situ, and operando study using infrared spectroscopy," J. Phys. Chem. C **127**, 14023 (2023).
[40]C. C. Li, Y. Sakata, T. Arai, K. Domen, K. Maruya, and T. Onishi, "Carbon monoxide and carbon dioxide adsorption on cerium oxide studied by Fourier-transform infrared spectroscopy. Part 1.—Formation of carbonate species on dehydroxylated CeO_2, at room temperature," J. Chem. Soc., Faraday Trans. 1 **85**, 929 (1989).
[41]C. Li, Y. Sakata, T. Arai, K. Domen, K. Maruya, and T. Onishi, "Adsorption of carbon monoxide and carbon dioxide on cerium oxide studied by Fourier-transform infrared spectroscopy. Part 2.—Formation of formate species on partially reduced CeO_2 at room temperature," J. Chem. Soc., Faraday Trans. 1 **85**, 1451 (1989).
[42]C. Binet, M. Daturi, and J.-C. Lavalley, "IR study of polycrystalline ceria properties in oxidised and reduced states," Catal. Today **50**, 207 (1999).
[43]Z. Yang, T. K. Woo, and K. Hermansson, "Strong and weak adsorption of CO on CeO_2 surfaces from first principles calculations," Chem. Phys. Lett. **396**, 384 (2004).
[44]B. W. J. Chen, L. Xu, and M. Mavrikakis, "Computational methods in heterogeneous catalysis," Chem. Rev. **121**, 1007 (2021).
[45]M. V. Ganduglia-Pirovano, A. Hofmann, and J. Sauer, "Oxygen vacancies in transition metal and rare earth oxides: Current state of understanding and remaining challenges," Surf. Sci. Rep. **62**, 219 (2007).
[46]P. Pérez-Bailac, P. G. Lustemberg, and M. V. Ganduglia-Pirovano, "Facet-dependent stability of near-surface oxygen vacancies and excess charge localization at CeO_2 surfaces," J. Phys.: Condens. Matter **33**, 504003 (2021).
[47]P. G. Lustemberg, P. N. Plessow, Y. Wang, C. Yang, A. Nefedov, F. Studt, C. Wöll, and M. V. Ganduglia-Pirovano, "Vibrational frequencies of cerium-oxide-bound CO: A challenge for conventional DFT methods," Phys. Rev. Lett. **125**, 256101 (2020).
[48]P. G. Lustemberg, C. Yang, Y. Wang, C. Wöll, and M. V. Ganduglia-Pirovano, "Vibrational frequencies of CO bound to all three low-index cerium oxide surfaces: A consistent theoretical description of vacancy-induced changes using density functional theory," J. Chem. Phys. **159**, 034704 (2023).
[49]V. Ganduglia-Pirovano, A. Martínez-Arias, S. Chen, Y. Wang, and P. G. Lustemberg, "Comment on 'surface characterization of cerium oxide catalysts using deep learning with infrared spectroscopy of CO,'" Mater. Today Sustainability **26**, 100783 (2024).

[50]E. Voloshina and B. Paulus, "Influence of electronic correlations on the ground-state properties of cerium dioxide," J. Chem. Phys. **124**, 234711 (2006).
[51]C. Müller, B. Paulus, and K. Hermansson, "Ab initio calculations of CO physisorption on ceria(111)," Surf. Sci. **603**, 2619 (2009).
[52]C. Müller, C. Freysoldt, M. Baudin, and K. Hermansson, "An ab initio study of CO adsorption on ceria(110)," Chem. Phys. **318**, 180 (2005).
[53]B. Herschend, M. Baudin, and K. Hermansson, "Electronic structure of CeO_2(110) surface oxygen vacancy," Surf. Sci. **599**, 173 (2005).
[54]B. Herschend, M. Baudin, and K. Hermansson, "CO adsorption on CeO_2(110) using hybrid-DFT embedded-cluster calculations," Chem. Phys. **328**, 345 (2006).
[55]B. Herschend, M. Baudin, and K. Hermansson, "Oxygen vacancy formation for transient structures on the CeO_2(110) surface at 300 and 750 K," J. Chem. Phys. **126**, 234706 (2007).
[56]C. Müller, B. Herschend, K. Hermansson, and B. Paulus, "Application of the method of increments to the adsorption of CO on the CeO_2(110) surface," J. Chem. Phys. **128**, 214701 (2008).
[57]H. Stoll, "On the correlation energy of graphite," J. Chem. Phys. **97**, 8449 (1992).
[58]H. Stoll, "The correlation energy of crystalline silicon," Chem. Phys. Lett. **191**, 548 (1992).
[59]H. Stoll, "Correlation energy of diamond," Phys. Rev. B **46**, 6700 (1992).
[60]T. Gruber, K. Liao, T. Tsatsoulis, F. Hummel, and A. Grüneis, "Applying the coupled-cluster ansatz to solids and surfaces in the thermodynamic limit," Phys. Rev. X **8**, 021043 (2018).
[61]I. Y. Zhang and A. Grüneis, "Coupled cluster theory in materials science," Front. Mater. **6**, 123 (2019).
[62]V. A. Neufeld, H.-Z. Ye, and T. C. Berkelbach, "Ground-state properties of metallic solids from *ab initio* coupled-cluster theory," J. Phys. Chem. Lett. **13**, 7497 (2022).
[63]M. C. Payne, M. P. Teter, D. C. Allen, T. A. Arias, and J. D. Joannopoulos, "Iterative minimization techniques for *ab initio* total-energy calculations: Molecular dynamics and conjugate gradients," Rev. Mod. Phys. **64**, 1045 (1992).
[64]G. Kresse and J. Furthmüller, "Efficient iterative schemes for *ab initio* total-energy calculations using a plane-wave basis set," Phys. Rev. B **54**, 11169 (1996).
[65]G. Kresse and J. Hafner, "*Ab initio* molecular dynamics for liquid metals," Phys. Rev. B **47**, 558 (1993).
[66]J. Wellendorff, K. T. Lundgaard, A. Møgelhøj, V. Petzold, D. D. Landis, J. K. Nørskov, T. Bligaard, and K. W. Jacobsen, "Density functionals for surface science: Exchange-correlation model development with Bayesian error estimation," Phys. Rev. B **85**, 235149 (2012).
[67]J. Perdew, K. Burke, and M. Ernzerhof, "Generalized gradient approximation made simple," Phys. Rev. Lett. **77**, 3865 (1996).
[68]S. L. Dudarev, G. A. Botton, S. Y. Savrasov, C. J. Humphreys, and A. P. Sutton, "Electron-energy-loss spectra and the structural stability of nickel oxide: An LSDA+U study," Phys. Rev. B **57**, 1505 (1998).
[69]J. Heyd, G. E. Scuseria, and M. Ernzerhof, "Hybrid functionals based on a screened Coulomb potential," J. Chem. Phys. **118**, 8207 (2003).
[70]J. Heyd, G. E. Scuseria, and M. Ernzerhof, "Erratum: 'Hybrid functionals based on a screened Coulomb potential' [J. Chem. Phys. 118, 8207 (2003)]," J. Chem. Phys. **124**, 219906 (2006).
[71]A. V. Krukau, O. A. Vydrov, A. F. Izmaylov, and G. E. Scuseria, "Influence of the exchange screening parameter on the performance of screened hybrid functionals," J. Chem. Phys. **125**, 224106 (2006).
[72]J. L. F. Da Silva, M. V. Ganduglia-Pirovano, J. Sauer, V. Bayer, and G. Kresse, "Hybrid functionals applied to rare-earth oxides: The example of ceria," Phys. Rev. B **75**, 045121 (2007).
[73]D. Du, M. J. Wolf, K. Hermansson, and P. Broqvist, "Screened hybrid functionals applied to ceria: Effect of Fock exchange," Phys. Rev. B **97**, 235203 (2018).
[74]M. V. Ganduglia-Pirovano, J. L. F. Da Silva, and J. Sauer, "Density-functional calculations of the structure of near-surface oxygen vacancies and electron localization on CeO_2(111)," Phys. Rev. Lett. **102**, 026101 (2009).
[75]H. J. Monkhorst and J. D. Pack, "Special points for Brillouin-zone integrations," Phys. Rev. B **13**, 5188 (1976).
[76]TURBOMOLE V 7.7.1 2017, a development of University of Karlsruhe and Forschungszentrum Karlsruhe GmbH, 1989-2007, TURBOMOLE GmbH, since 2007, http://www.turbomole.com.
[77]C. Møller and M. Plesset, "Note on an approximation treatment for many-electron systems," Phys. Rev. **46**, 618 (1934).
[78]K. Raghavachari, G. Trucks, J. Pople, and M. Head-Gordon, "A fifth-order perturbation comparison of electron correlation theories," Chem. Phys. Lett. **157**, 479 (1989).
[79]F. Weigend and R. Ahlrichs, "Balanced basis sets of split valence, triple zeta valence and quadruple zeta valence quality for H to Rn: Design and assessment of accuracy," Phys. Chem. Chem. Phys. **7**, 3297 (2005).
[80]R. Gulde, P. Pollak, and F. Weigend, "Error-balanced segmented contracted basis sets of double-ζ to quadruple-ζ valence quality for the lanthanides," J. Chem. Theory Comput. **8**, 4062 (2012).
[81]D. Rappoport and F. Furche, "Property-optimized Gaussian basis sets for molecular response calculations," J. Chem. Phys. **133**, 134105 (2010).
[82]D. Rappoport, "Property-optimized Gaussian basis sets for lanthanides," J. Chem. Phys. **155**, 124102 (2021).
[83]F. Weigend, M. Häser, H. Patzelt, and R. Ahlrichs, "RI-MP2: Optimized auxiliary basis sets and demonstration of efficiency," Chem. Phys. Lett. **294**, 143 (1998).
[84]A. Hellweg, C. Hättig, S. Höfener, and W. Klopper, "Optimized accurate auxiliary basis sets for RI-MP2 and RI-CC2 calculations for the atoms Rb to Rn," Theor. Chem. Acc. **117**, 587 (2007).
[85]J. Chmela and M. E. Harding, "Optimized auxiliary basis sets for density fitted post-Hartree–Fock calculations of lanthanide containing molecules," Mol. Phys. **116**, 1523 (2018).
[86]G. L. Stoychev, A. A. Auer, and F. Neese, "Automatic generation of auxiliary basis sets," J. Chem. Theory Comput. **13**, 554 (2017).
[87]M. Dolg, H. Stoll, and H. Preuss, "Energy-adjusted *ab initio* pseudopotentials for the rare earth elements," J. Chem. Phys. **90**, 1730 (1989).
[88]K. A. Peterson and T. H. J. Dunning, "Accurate correlation consistent basis sets for molecular core–valence correlation effects: The second row atoms Al–Ar, and the first row atoms B–Ne revisited," J. Chem. Phys. **117**, 10548 (2002).
[89]Q. Lu and K. A. Peterson, "Correlation consistent basis sets for lanthanides: The atoms La–Lu," J. Chem. Phys. **145**, 054111 (2016).
[90]C. Hättig, "Optimization of auxiliary basis sets for RI-MP2 and RI-CC2 calculations: Core–valence and quintuple-ζ basis sets for H to Ar and QZVPP basis sets for Li to Kr," Phys. Chem. Chem. Phys. **7**, 59 (2005).
[91]V. Rokhlin, "Rapid solution of integral equations of classical potential theory," J. Comput. Phys. **60**, 187 (1985).
[92]L. Greengard, "The rapid evaluation of potential fields in particle systems," Ph.D. thesis, Department of Computer Science, Yale University, 1987.
[93]C. A. White and M. Head-Gordon, "Derivation and efficient implementation of the fast multipole method," J. Chem. Phys. **101**, 6593 (1994).
[94]C. G. Lambert, T. A. Darden, and J. A. Board, Jr., "Multipole-based algorithm for efficient calculation of forces and potentials in macroscopic periodic assemblies of particles," J. Comput. Chem. **126**, 274 (1996).
[95]K. N. Kudin and G. E. Scuseria, "A fast multipole method for periodic systems with arbitrary unit cell geometries," Chem. Phys. Lett. **283**, 61 (1998).
[96]K. N. Kudin and G. E. Scuseria, "Revisiting infinite lattice sums with the periodic fast multipole method," J. Chem. Phys. **121**, 2886 (2004).
[97]U. Wedig, Ph.D. thesis, Karlsruher Intitut für Technologie, 1986.
[98]The results obtained with the PEECM method were contrasted in some cases with those resulting from a tailor-made point charge field that met the condition of a zero dipole moment. It was found that both embedding models converge to the same results when using tailor-made point charge fields with more than 21 200 charges.
[99]T. H. Dunning, Jr., "Gaussian basis sets for use in correlated molecular calculations. I. The atoms boron through neon and hydrogen," J. Chem. Phys. **90**, 1007 (1989).
[100]J. Gauss and J. F. Stanton, "Analytic CCSD(T) second derivatives," Chem. Phys. Lett. **276**, 70 (1997).

[101]J. F. Stanton, J. Gauss, L. Cheng, M. E. Harding, D. A. Matthews, P. G. Szalay, "CFOUR, Coupled-Cluster techniques for Computational Chemistry, a quantum-chemical program package," with contributions from A. Asthana, A. A. Auer, R. J. Bartlett, U. Benedikt, C. Berger, D. E. Bernholdt, S. Blaschke, Y. J. Bomble, S. Burger, O. Christiansen, D. Datta, F. Engel, R. Faber, J. Greiner, M. Heckert, O. Heun, M. Hilgenberg, C. Huber, T.-C. Jagau, D. Jonsson, J. Jusélius, T. Kirsch, M.-P. Kitsaras, K. Klein, G. M. Kopper, W. J. Lauderdale, F. Lipparini, J. Liu, T. Metzroth, L. A. Mück, D. P. O'Neill, T. Nottoli, J. Oswald, D. R. Price, E. Prochnow, C. Puzzarini, K. Ruud, F. Schiffmann, W. Schwalbach, C. Simmons, S. Stopkowicz, A. Tajti, T. Uhlířová, J. Vázquez, F. Wang, J. D. Watts, P. Y. C. Zhang, X. Zheng, the integral packages MOLECULE (J. Almlöf, P. R. Taylor), PROPS (P. R. Taylor), ABACUS (T. Helgaker, H. J. A. Jensen, P. Jørgensen, J. Olsen), ECP routines by A. V. Mitin, and C. van Wüllen, For the current version, see http://www.cfour.de..

[102]J. Vázquez, M. E. Harding, J. F. Stanton, and J. Gauss, "Vibrational energy levels via finite-basis calculations using a quasi-analytic form of the kinetic energy," J. Chem. Theory Comput. **7**, 1428 (2011).

[103]Z. Yang, T. K. Woo, M. Baudin, and K. Hermansson, "Atomic and electronic structure of unreduced and reduced CeO_2 surfaces: A first-principles study," J. Chem. Phys. **120**, 7741 (2004).

[104]N. V. Skorodumova, M. Baudin, and K. Hermansson, "Surface properties of CeO_2 from first principles," Phys. Rev. B **69**, 075401 (2004).

[105]Y. Jiang, J. B. Adams, and M. van Schilfgaarde, "Density-functional calculation of CeO_2 surfaces and prediction of effects of oxygen partial pressure and temperature on stabilities," J. Chem. Phys. **123**, 064701 (2005).

[106]K. P. Huber and G. H. Herzberg, "Constants of diatomic molecules," in *NIST Chemistry WebBook, NIST Standard Reference Database Number 69*, edited by P. J. Linstrom and W. G. Mallard (National Institute of Standards and Technology No. 69, Gaithersburg, MD, 2024).

[107]D. P. Tew, W. Klopper, M. Heckert, and J. Gauss, "Basis set limit CCSD(T) harmonic vibrational frequencies," J. Phys. Chem. A **111**, 11242 (2007).

[108]C. Yang, L.-L. Yin, F. Bebensee, M. Buchholz, H. Sezen, S. Heissler, J. Chen, A. Nefedov, H. Idriss, X.-Q. Gong, and C. Wöll, "Chemical activity of oxygen vacancies on ceria: A combined experimental and theoretical study on CeO_2(111)," Phys. Chem. Chem. Phys. **16**, 24165 (2014).

[109]C. Yang, X. Yu, S. Heißler, A. Nefedov, S. Colussi, J. Llorca, A. Trovarelli, Y. Wang, and C. Wöll, "Surface faceting and reconstruction of ceria nanoparticles," Angew. Chem., Int. Ed. **56**, 375 (2017).

[110]N. C. Handy, J. F. Gaw, and E. D. Simandiras, "Accurate *ab initio* of molecular geometries and spectroscopic constants, using SCF and MP2 energy derivatives," J. Chem. Soc., Faraday Trans. 2 **83**, 1577 (1987).

[111]G. Spoto, E. Gribov, A. Damin, G. Ricchiardi, and A. Zecchina, "The IR spectra of Mg_{5C}^{2+}(CO) complexes on the (001) surfaces of polycrystalline and single crystal MgO," Surf. Sci. **540**, L605 (2003).

[112]H.-Z. Ye and T. C. Berkelbach, "Adsorption and vibrational spectroscopy of CO on the surface of MgO from periodic local coupled-cluster theory," Faraday Discuss. **254**, 628 (2024).

[113]S. F. Boys and F. Bernardi, "The calculation of small molecular interactions by the differences of separate total energies. Some procedures with reduced errors," Mol. Phys. **19**, 553 (1970).

[114]M. Nolan, S. C. Parker, and G. W. Watson, "Vibrational properties of CO on ceria surfaces," Surf. Sci. **600**, L175 (2006).

[115]L. A. Burns, M. S. Marshall, and C. D. Sherrill, "Comparing counterpoise-corrected, uncorrected, and averaged binding energies for benchmarking noncovalent interactions," J. Chem. Theory Comput. **10**, 49 (2014).

[116]B. Brauer, M. K. Kesharwani, and J. M. L. Martin, "Some observations on counterpoise corrections for explicitly correlated calculations on noncovalent interactions," J. Chem. Theory Comput. **10**, 3791 (2014).

[117]F. Jensen, "Basis set superposition errors are partly basis set imbalances," J. Chem. Theory Comput. **20**, 767 (2024).

[118]T. M. Henderson, J. Paier, and G. E. Scuseria, "Accurate treatment of solids with the HSE screened hybrid," Phys. Status Solidi B **248**, 767 (2011).

[119]H. D. Saßnick and C. Cocchi, "Electronic structure of cesium-based photocathode materials from density functional theory: Performance of PBE, SCAN, and HSE06 functionals," Electron. Struct. **3**, 027001 (2021).